Triplet-State Chemiluminescence: Acetone T_1 from the Decomposition of Chemically Activated 3,3-Dimethyl-4-(*N*,*N*-dimethylamino)-1,2-dioxetane

Denis J. Bogan* and Dong-Heon Lee

Department of Chemistry, The Catholic University of America, Washington, DC 20064

(Received: November 19, 1990)

The reaction of $O_2(a,{}^1\Delta_g)$ with *N*,*N*-dimethylisobutenylamine has been studied in the gas phase at 298 K, a total pressure of 4 Torr, and an oxygen partial pressure of 0.007–4.0 Torr. The reaction forms a chemically activated dioxetane that decomposes with chemiluminescence (CL). CL spectra were obtained, and deconvolution showed them to consist of acetone $T_1 \rightarrow S_0$ and $S_1 \rightarrow S_0$ and no other molecular emissions. The T_1 state was efficiently quenched by O_2. The integrated intensity ratio, $I(T_1)/I(S_1)$, was 1.3 at $P(O_2) = 0$. The $T_1 \rightarrow S_0$ spectrum shows its onset at 366 nm and peak intensity at 440 nm.

Introduction

The 1,2-dioxetanes are well-known to give carbonyl $n\pi^*$ excited states upon unimolecular fragmentation.[1-4] Most reported work has been done by thermal decomposition of the dioxetane in inert solvent using fluorescence sensitizing agents, such as 9,10-diphenylanthracene, to count singlet (S_1) products and phosphorescence sensitizers, such as 9,10-dibromoanthracene, to count triplet (T_1) products. The yields of T_1 considerably exceed the yields of S_1.[1a] For the prototype tetramethyldioxetane molecule, the initial concentration ratio, $[T_1]/[S_1] = 140$, has been reported.[1a] The Arrhenius activation energies for dioxetane thermal chemiluminescent decomposition are typically 25 ± 5 kcal/mol.[1]

Many 1,2-dioxetanes have been made in the gas phase by the cycloaddition reactions of olefins with $O_2({}^1\Delta)$.[4] Most of these cycloadditions have activation energies of 15 ± 5 kcal/mol. The initially formed dioxetanes are chemically activated, having ≥ 50 kcal/mol of vibrational–rotational energy. Their lifetimes are $\leq 10^{-8}$ s for the reactions we have reported. Discharge flow reactor techniques and chemiluminescence (CL) spectroscopy were used for our previous work[4] and the present work.

In this paper we report the investigation of a reaction of the above type, $O_2(a,{}^1\Delta_g)$ plus *N*,*N*-dimethylisobutenylamine at 298 K and a total pressure of 4 Torr. In a previous CL study of this reaction, pure oxygen at 4 Torr was the discharged gas.[4b] In the present work, the discharged gas was a mixture of helium and oxygen at a total pressure of 4 Torr. The oxygen partial pressure was varied from 0.007 to 0.66 Torr. Oxygen cannot be eliminated because it is the source of the $O_2(a,{}^1\Delta_g)$ reactant. Both S_1 and T_1 states of acetone are expected to be present as reaction products. Ground-state $O_2(X,{}^3\Sigma_g^-)$ is an efficient quencher of the acetone T_1 state.[7b] The previously observed CL spectrum consisted of acetone S_1–S_0 exclusively.[4b] The CL spectra observed in the present work showed a distinct shift to the red that increased with decreasing oxygen concentration. The S_1–S_0 component was subtracted from the spectra, leaving pure acetone T_1–S_0 emission. We report the T_1–S_0 CL spectrum and a plot of the quenching of the T_1 state by oxygen.

It is significant that the reaction of *N*,*N*-dimethylisobutenylamine with $O_2({}^1\Delta)$ has been studied under single-collision conditions using crossed molecular beams.[5] CL was observed, providing conclusive proof that the process is a chemically activated unimolecular reaction. The activated intermediate is 3,3-dimethyl-4-(*N*,*N*-dimethylamino)-1,2-dioxetane. CL occurred at line-of-centers collision energies of 4–9 kcal/mol.[5] Reaction 1

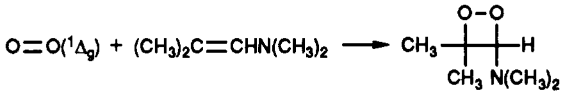

$$O{=}O({}^1\Delta_g) + (CH_3)_2C{=}CHN(CH_3)_2 \longrightarrow CH_3C(CH_3)(O{-})\!-\!CH(N(CH_3)_2)(O{-}) \quad (1)$$

has been proposed as the initial step in the photosensitized oxygenation of *N*,*N*-dimethylisobutenylamine.[16] The final products of the reaction were acetone and *N*,*N*-dimethylformamide.[16] Later, an NMR spectrum and a molecular weight determination were reported as evidence that 3,3-dimethyl-4-(*N*,*N*-dimethylamino)-1,2-dioxetane is the intermediate in the overall reaction.[17]

Experimental Section

The experimental procedure for this work was essentially the same as that used previously.[4] Full experimental details and schematic diagrams of the apparatus and the potential energy surface for the reaction have been published.[4a,b] Helium and oxygen were mixed on-line upstream of the microwave discharge. A ring of HgO, deposited on the discharge tube immediately downstream from the microwave cavity, catalyzed the recombination of atomic oxygen to $O_2({}^1\Delta)$. Olefin was vaporized from

---

[1] (a) Adam, W. In *Chemical and Biological Generation of Excited States*; Adam, W., Cilento, G., Eds.; Academic Press: New York, 1982; pp 115-52. (b) Baumstark, A. L. *Adv. Oxygenated Processes* **1988**, *1*, 31-84. (c) Turro, N. J.; Lechtken, P.; Schore, N. E.; Schuster, G.; Steinmetzer, H.-C.; Yekta, A. *Acc. Chem. Res.* **1974**, *7*, 97-105.

[2] (a) Baumstark, A. L.; Retter, C. A.; Tehrani, K.; Kellogg, C. *J. Org. Chem.* **1987**, *52*, 3308-11. (b) Richardson, W. H.; Stiggal-Estberg, D. L.; Chen, Z.; Baker, J. C.; Burns, D. M.; Sherman, D. G. *J. Org. Chem.* **1987**, *52*, 3143-50. (c) Baumstark, A. L.; Niroomand, F.; Vasquez, P. C. *J. Org. Chem.* **1984**, *49*, 4497-500. (d) Adam, W.; Baader, W. J. *J. Am. Chem. Soc.* **1985**, *107*, 410.

[3] (a) Tolbert, M. A.; Huestis, D. L.; Rossi, M. J. *J. Phys. Chem.* **1988**, *92*, 4094-9. (b) Chowdhury, P. K.; Pola, J.; Rao, K. V. S. R.; Mittal, J. P. *Chem. Phys. Lett.* **1987**, *142*, 252-4. (c) McGinley, E. S.; Crim, F. F. *J. Chem. Phys.* **1986**, *85*, 5741-7. (d) Ruhman, S.; Anner, O.; Haas, Y. *Faraday Discuss. Chem. Soc.* **1983**, *75*, 239-50. (e) West, G. A.; Mariella, R. P.; Pete, J. A.; Hammond, W. B. *J. Chem. Phys.* **1981**, *75*, 2006-7.

[4] (a) Bogan, D. J. In *Chemical and Biological Generation of Excited States*; Adam, W., Cilento, G., Eds.; Academic Press: New York, 1982; pp 37-83. (b) Bogan, D. J.; Durant, J. L.; Sheinson, R. S.; Williams, F. W. *Photochem. Photobiol.* **1979**, *30*, 3. (c) Bogan, D. J.; Sheinson, R. S.; Gann, R. G.; Williams, F. W. *J. Am. Chem. Soc.* **1975**, *97*, 2560. (d) Bogan, D. J.; Sheinson, R. S.; Williams, F. W. *J. Am. Chem. Soc.* **1976**, *98*, 1034.

[5] Alben, K. T.; Auerbach, A.; Ollison, W. M.; Weiner, J.; Cross, R. J. *J. Am. Chem. Soc.* **1978**, *100*, 3274.

[6] Hodgeman, C. D., Ed. *Handbook of Chemistry and Physics*, 41st ed.; Chemical Rubber Publishing Co.: Cleveland, OH, 1959; p 2798.

[7] (a) Turro, N. J. *Modern Molecular Photochemistry*; Benjamin/Cummings: Menlo Park, CA, 1978; p 189. (b) *Ibid.*, p 354.

[8] (a) Chandler, W. D.; Goodman, L. *J. Mol. Spectrosc.* **1970**, *36*, 141. (b) O'Sullivan, M.; Testa, A. C. *J. Am. Chem. Soc.* **1970**, *92*, 258.

[9] Gehrtz, M.; Brauchle, Chr.; Voitlander, J. *Mol. Phys.* **1984**, *53*, 769.

[10] Luntz, A. C.; Maxson, V. T. *Chem. Phys. Lett.* **1974**, *26*, 553.

[11] (a) Cundall, R. B.; Davies, A. S. *Proc. R. Soc. London* **1966**, *A290*, 563. (b) McGlynn, S. P.; Azumi, T.; Kinoshita, M. *The Triplet State*; Prentice-Hall: Englewood Cliffs, NJ, 1969; p 242.

[12] Copeland, R. A.; Crosley, D. R. *Chem. Phys. Lett.* **1985**, *115*, 362.

[13] Gilmore, E. H.; Gibson, G. E.; McClure, D. S. *J. Chem. Phys.* **1952**, *20*, 829.

[14] Greenblatt, G. D.; Ruhman, S.; Haas, Y. *Chem. Phys. Lett.* **1984**, *112*, 200.

[15] Strickler, S. J.; Berg, R. A. *J. Chem. Phys.* **1962**, *37*, 814.

[16] Foote, C. S.; Lin, J. W.-P. *Tetrahedron Lett.* **1968**, 3267.

[17] Foote, C. S.; Dzakpasu, A. A.; Lin, J. W.-P. *Tetrahedron Lett.* **1975**, 1247.

0022-3654/91/2095-1533$02.50/0 © 1991 American Chemical Society

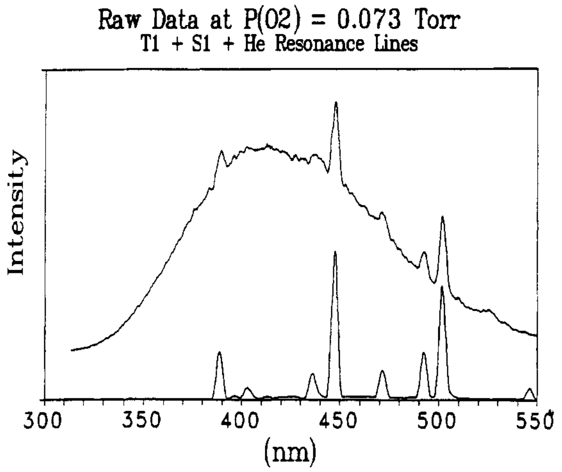

Figure 1. Typical raw CL spectrum. The spectrum of discharged helium is shown in the lower trace. Weak Hg lines at 404, 436, and 546 nm are also present in the lower trace.

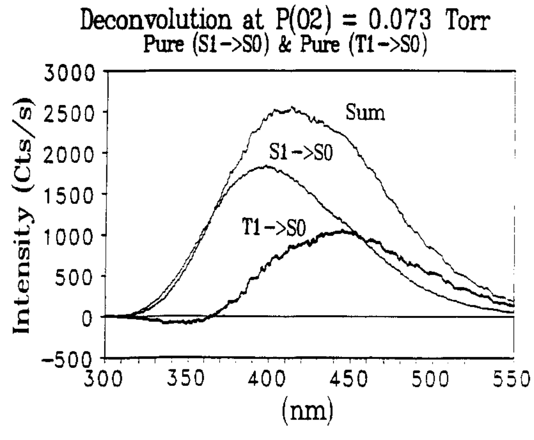

Figure 2. Typical spectral deconvolution. The upper trace is the spectrum of Figure 1 with the He lines truncated. The middle trace is $S_1 \rightarrow S_0$. The lower bold trace is the difference between the other two and is attributed to $T_1 \rightarrow S_0$. The integrated intensity ratio $I(T_1)/I(S_1) = 0.56$.

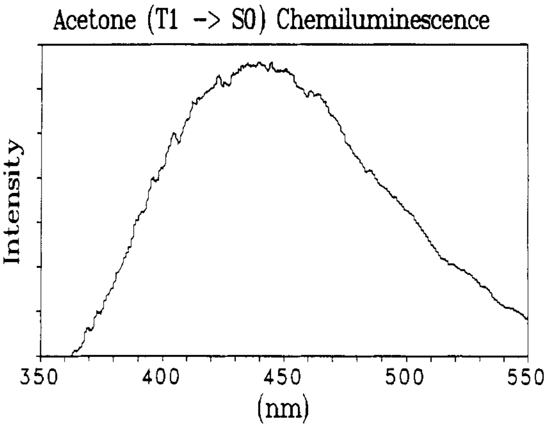

Figure 3. Composite acetone ($T_1 \rightarrow S_0$) CL spectrum. The peak intensity is 13 000 counts/s at 440 nm.

a liquid reservoir at 273 K and introduced at a partial pressure of 0.012 Torr through an on-axis probe located at the upstream end of the observed reactor volume. The bulk flow velocity was 10–20 m/s. The $^1/_2$-m $f/6.9$ monochromator was driven by a computer-controlled stepper motor. The photomultiplier tube, a Hamamatsu R1527P operated at 258 K with single-photon counting electronics, had an average dark count of 0.5/s. The raw spectra, representing plots of photon counts/s vs 1024 channels, were subjected to five-point smoothing. Wavelength calibration was done with He and Hg atomic lines.

The product CL spectrum taken with an oxygen partial pressure of 0.66 Torr was compared to the 4-Torr spectrum and showed a small red shift. Thirteen CL spectra were taken with oxygen partial pressures of 0.007–0.66 Torr, a range of a factor of 100. The spectra showed an increase in the red shift with decreasing oxygen pressure. Well-known atomic helium resonance lines at wavelengths of 389, 403, 439, 447, 492, 502, and 588 nm[6] also appeared with increasing intensity as oxygen pressure was decreased. These were easily identified by their triangular shapes, with width at half-height = 3.4 nm = spectral slit width, and were truncated, leaving smooth spectral envelopes. A typical raw spectrum and the spectrum of pure discharged He are shown in Figure 1.

The next step was to subtract the contribution of $S_1 \rightarrow S_0$ emission and to determine whether the remainder could be assigned to $T_1 \rightarrow S_0$. A spectrum taken with 4 Torr of pure discharged oxygen was used as the reference ($S_1 \rightarrow S_0$) emission. The quenching plot given below (Figure 4) justifies the assumption that the reference spectrum was pure $S_1 \rightarrow S_0$. A normalization coefficient was determined representing the fractional contribution of $S_1 \rightarrow S_0$ in the spectrum. The zero-point vibrational energy level of the T_1 state lies 78 kcal/mol above the ground state,[7a] corresponding to 366 nm. One-half of the spectral slit width at its base was 3 nm. The normalization coefficient for the S_1 component was chosen so that the onset of the residual spectrum was 363 nm. This criterion was followed for all spectra; no other adjustments were made. Figure 2 shows the results of applying this procedure to the upper spectrum in Figure 1. All of the deconvoluted spectra show a small unexplained negative residual to the blue of 363 nm, as does Figure 2.

Results and Discussion

Figure 3 shows the result of summing the residuals of the 13 deconvoluted spectra over the wavelength range 363–550 nm. As an average of all the data taken, it is of considerably higher quality than any one residual spectrum. Maximum intensity is at 440 nm. An estimated 5% of the emission occurs beyond 550 nm. Figure 3 is deemed to be pure acetone $T_1 \rightarrow S_0$ emission. It is in quantitative agreement with spectra taken in low-temperature solutions and glasses,[8] suggesting that the emitting T_1 molecules are relaxed to a thermal distribution. The spectral shape and the size of the Stokes shift bear a strong resemblance to those of acetone $S_1 \rightarrow S_0$, consistent with the large out-of-plane angle (reported to be 38°)[9] for the methyl groups in the T_1 state. This emission was quenched efficiently by $O_2(X,{}^3\Sigma_g^-)$.

Integrated intensity ratios, $I(T_1)/I(S_1)$, were obtained at each experimental oxygen pressure. To analyze these data, it was assumed that the only quenching process having a nonnegligible rate constant was that of T_1 by $O_2(X,{}^3\Sigma_g^-)$. Stern–Volmer analysis is applicable to quenching when there is a well-defined time of formation for the observed excited state. However, this condition was not satisfied in our steady-state flow reactor. The time of formation for an individual chemiexcited molecule is coincident with the reactive collision. CL was easily seen in the darkened room and filled the reactor homogeneously. This fact shows that there was a homogeneous density of reactive collisions throughout the observed volume and hence a broad distribution of excited product formation times. The mean residence time of gas in the 100-cm^3 reactor was approximately 2×10^{-2} s.

Under these conditions T_1 loss by quenching is given by

$$-d[T_1]/dt = k_Q[O_2][T_1] \quad \text{and} \quad \ln [T_1] = \ln [T_1]_0 - k_Q f(t)[O_2] \qquad (2)$$

where $P(O_2) = 0$ is denoted by subscript 0 and $f(t)$ is the distribution function for product formation times. We did not determine $f(t)$ explicitly, but it was the same for every spectrum since temperature, total pressure, and bulk flow velocity were constants. Assuming that $[S_1]$ is constant and that $I(T_1) \propto [T_1]$ and $I(S_1) \propto [S_1]$

$$\ln \{I(T_1)/I(S_1)\} = \ln \{I(T_1)/I(S_1)\}_0 - k_Q f(t) P(O_2) \qquad (3)$$

where $P(O_2)$ was taken as the measured partial pressure of oxygen entering the discharge. Figure 4 shows a quenching plot based

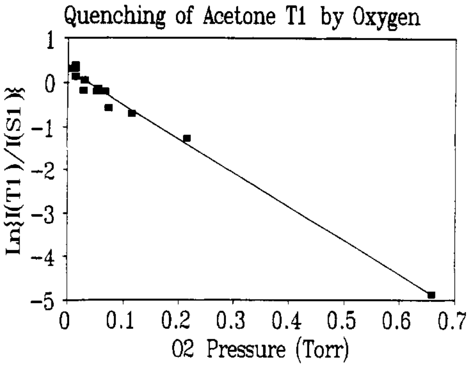

Figure 4. Plot of the quenching of acetone T_1 by oxygen.

upon eq 3. The intercept yields $\{I(T_1)/I(S_1)\}_0 = 1.31 \pm 0.07$. The least-squares analysis of Figure 4 shows that $\{I(T_1)/I(S_1)\}_0$ will be reduced to $1/e$ of its value by the addition of 0.137 ± 0.005 Torr of O_2. Combining this value with the assumption of hard-sphere (van der Waals radius) collisions of T_1 with $O_2(^3\Sigma)$ and a quenching probability of 1/3 per collision leads to a cross section of 40 Å^2 and a mean lifetime at $P(O_2) = 0$ of 1×10^{-6} s. The latter number is taken as the best estimate, for present purposes, of the phosphorescence lifetime, τ_P, at $P(O_2) = 0$, $P(\mathrm{He}) = 4$ Torr, P(*N,N*-dimethylisobutenylamine) = 0.012 Torr, and $T = 298$ K. For comparison, Luntz and Maxson observed a cross section of 22 ± 5 Å^2 for quenching of $D_2CO(T_1)$ by NO.[10]

Conversion of $I(T_1)/I(S_1)$ to the ratio of formation rate constants, k_{T_1}/k_{S_1}, requires the radiative lifetimes τ_{R,T_1} and τ_{R,S_1}. Making the steady-state assumption on T_1 concentration

$$0 = d[T_1]/dt = k_{T_1}[\text{olefin}][\Delta] - [T_1](k_R + k_{NR})$$

then

$$[T_1] = \frac{k_{T_1}[\text{olefin}][\Delta]}{k_R + k_{NR}} = \frac{k_{T_1}[\text{olefin}][\Delta]}{k_P}$$

$$I(T_1) = A_{T_1 \to S_0}[T_1] = \frac{A_{T_1 \to S_0} k_{T_1}[\text{olefin}][\Delta]}{k_P}$$

where Δ is $O_2(a,{}^1\Delta_g)$. The steady-state assumption on $[S_1]$ leads to analogous equations and to the expression

$$\frac{k_{T_1}}{k_{S_1}} = \frac{I(T_1) k_P A_{S_1 \to S_0}}{I(S_1) k_F A_{T_1 \to S_0}}$$

Using the standard notation, subscripts R and NR denote radiative and nonradiative transitions, respectively, $A_{X \to Y}$ is the Einstein coefficient for spontaneous emission from upper state X to lower state Y, and $k_P = k_R + k_{NR}$ is the unimolecular rate constant for deactivation of the phosphorescent state in the absence of quenching. The definitions $k = 1/\tau$ and $A_{X \to Y} = 1/\tau_{R,X}$ lead to the equation

$$\frac{k_{T_1}}{k_{S_1}} = \frac{I(T_1)\Phi_F}{I(S_1)\Phi_P} = \frac{I(T_1)\tau_F \tau_{R,T_1}}{I(S_1)\tau_P \tau_{R,S_1}} \qquad (4)$$

For the S_1 state, $\tau_F = 2.4 \times 10^{-9}$ s[18] and $\tau_{R,S_1} = 10 \times 10^{-6}$ s[14] are available. For T_1, our value of $\tau_P = 1 \times 10^{-6}$ s will be used, but τ_{R,T_1} is still needed. Published values of τ_{R,T_1} range from 0.2×10^{-3} to 20×10^{-3} s.[11] The zero-pressure lifetime of T_1 has recently been determined in the gas phase at 298 K.[12] A lifetime of 225×10^{-6} s was found for the thermalized T_1 state.[12] Radiationless deactivation can occur in the absence of collisions; thus $\tau_{R,T_1} \geq 225 \times 10^{-6}$ s. Using $\tau_{R,T_1} \geq 225 \times 10^{-6}$ s, $\tau_{R,S_1} = 10 \times 10^{-6}$ s, $\tau_P = 1 \times 10^{-6}$ s, and $\tau_F = 2.4 \times 10^{-9}$ s, and eq 4 yields $k_{T_1}/k_{S_1} \geq 0.07$.

This is not a very satisfying result. In the majority of studies of dioxetane thermal decomposition, $[T_1]/[S_1] \gg 1$ has been observed.[1,2] Reported examples where $S_1 > T_1$ are believed to proceed by electron-transfer mechanisms.[19] In this work both the chemically activated dioxetane (eq 1) and its decomposition products are nonionic. Intra- and intermolecular electron-transfer steps for decomposition of the chemically activated 3,3-dimethyl-4-(*N,N*-dimethylamino)-1,2-dioxetane are unlikely under the present experimental conditions.

The largest factor leading to uncertainty in k_{T_1}/k_{S_1} is the considerable uncertainty in the radiative lifetime of the T_1 state. $\tau_{R,T_1} = 0.02$ s has been reported in a solid solution at 77 K, conditions admittedly much different than the present ones.[13] Use of this value would yield $k_{T_1}/k_{S_1} = 6$. We do not recommend a value of k_{T_1}/k_{S_1} at this time.

The emission intensity ratio, $I(T_1)/I(S_1)$, reported here can stand on its own merits. A measurement of $A_{T_1 \to S_0}$ would significantly enhance the value of the present work because our results could then be converted to a reliable k_{T_1}/k_{S_1}. Since photon flux is the primary measured quantity in these experiments, it is crucial to have the Einstein A if possible, not a reciprocal lifetime. It would be desirable to obtain the needed value from the integrated absorption spectrum by using the Strickler–Berg formalism.[14,15]

In our previous report on this reaction a quantum yield for S_1 product of $4 \times 10^{-4} \pm$ a factor of 4 was given, based upon $\Phi_F = 10^{-3}$.[4b] This should be revised to $2 \times 10^{-3} \pm$ a factor of 4, based upon the value of $\Phi_F = 2.4 \times 10^{-4}$ used here. Our published quantum yields for reactions giving formaldehyde S_1 product are unaffected.

The ability to observe directly both $S_1 \to S_0$ and $T_1 \to S_0$ CL spectra in reactions of this type is an important advance because it will facilitate studies of product energy partitioning. Previously, we were limited to the comparison of S_1 quantum yields for differently substituted dioxetanes. It is likely that the large internal energy associated with the chemical activation process will result in a lower selectivity for T_1 than observed in thermal dioxetane decomposition. Further work is in progress.

Acknowledgment. We thank the Catholic University of America for a start-up grant and Dr. R. D. Johnson for writing a computer program to read our spectral data files into a spreadsheet.

---

[18] Halpern, A. M.; Ware, W. R. *J. Chem. Phys.* **1971**, *54*, 1271.

[19] See for example: (a) Schuster, G. B.; Dixon, B.; Koo, J.-Y.; Schmidt, S. P.; Smith, J. P. *Photochem. Photobiol.* **1979**, *30*, 17. (b) Schaap, A. P.; Gagnon, S. D. *J. Am. Chem. Soc.* **1982**, *104*, 3504.